Magnetoelectric susceptibility and magnetic symmetry of magnetoelectrically annealed $TbPO_4$

G. T. Rado,* J. M. Ferrari, and W. G. Maisch
Naval Research Laboratory, Washington, D.C. 20375
(Received 3 October 1983)

Measurements are presented of the magnetoelectric (ME) susceptibility tensor $\overleftrightarrow{\alpha}$ of $TbPO_4$ crystals which were ME annealed by a method introduced in the present paper and termed "balanced" ME annealing. The form of $\overleftrightarrow{\alpha}$ shows that below the Néel temperature the magnetic symmetry of such crystals is tetragonal (point group $4'/m'mm'$), in contrast to the lower symmetry which describes non-ME-annealed $TbPO_4$ crystals. Thus the distortion existing in the latter crystals is suppressed by ME annealing. Also measured are the magnitude (which is larger than in any other known material) and temperature dependence of the single independent component of $\overleftrightarrow{\alpha}$. The improved experimental methods presented include, besides the balanced ME annealing, the simultaneous observation of two components of $\overleftrightarrow{\alpha}$, and a modified procedure for the growth of $TbPO_4$ crystals. Magnetoelectric switching, memory, and hysteresis effects are also reported.

I. INTRODUCTION

In this paper we report on experimental investigations of magnetoelectric (ME) effects in single crystals of antiferromagnetic terbium phosphate ($TbPO_4$). The motivation for the work was twofold. Firstly, the linear ME effect in $TbPO_4$ is an order of magnitude larger than that in any other material, as first reported by us at the 1972 Conference on Magnetism and Magnetic Materials.[1] To the best of our knowledge no material possessing a larger ME susceptibility has been discovered since then. The existence of ME effects in $TbPO_4$ was subsequently verified by England.[2]

Our early experimental results[1] are described in Sec. II of this paper and include the ME annealing used to eliminate antiferromagnetic domains, a partial determination of the form of $\overleftrightarrow{\alpha}$, and the temperature dependence and magnitude of a certain component of $\overleftrightarrow{\alpha}$. Some theoretical considerations on the atomic mechanism of $\overleftrightarrow{\alpha}$ in $TbPO_4$ are also presented. This is followed by an account of our observations of switching, memory, and hysteresis effects exhibited by $\overleftrightarrow{\alpha}$ when a $TbPO_4$ crystal is subjected to a biasing magnetic field.

The second motivation for our work was the need to establish unambiguously the magnetic symmetry of magnetoelectrically annealed (henceforth referred to as "ME-annealed") $TbPO_4$. While we were able to conclude from our earlier experiments[1] that the magnetic symmetry of non-ME-annealed $TbPO_4$ is lower than tetragonal, the experimental data on ME-annealed $TbPO_4$ included only six of the nine components of $\overleftrightarrow{\alpha}$, so that the magnetic symmetry of ME-annealed $TbPO_4$ could not be determined. The unavailability of crystals from which samples having adequate faces perpendicular to all three tetragonal axes could be fashioned prevented us from measuring the remaining three components of $\overleftrightarrow{\alpha}$ in our earlier work. Recently we obtained suitable crystals which enabled us to measure all nine components of $\overleftrightarrow{\alpha}$.

As presented[3] (but not published) at the 1982 Joint Intermag-Magnetism and Magnetic Materials Conference and described in Sec. III of this paper, we used improved experimental methods including "balanced" ME annealing, the simultaneous observation of two components of $\overleftrightarrow{\alpha}$, and a modified procedure for the growth of $TbPO_4$ crystals. By means of these methods and the new crystals we determined the form of $\overleftrightarrow{\alpha}$ completely. In this way we found that in properly ME-annealed $TbPO_4$ the magnetic symmetry is tetragonal with point group $4'/m'mm'$, just as in $DyPO_4$, and thus higher than the magnetic symmetry of non-ME-annealed $TbPO_4$. It is non-ME-annealed $TbPO_4$ which has been used for all neutron-diffraction[4] and other non-ME experiments performed on $TbPO_4$ to date.

II. ME SUSCEPTIBILITY

A. ME annealing and partial determination of $\overleftrightarrow{\alpha}$

We recall that $\overleftrightarrow{\alpha}$ is defined by

$$F=-\alpha_{ij}E_iH_j\ , \tag{1}$$

where F is the ME contribution to the free-energy density, and E_i and H_j are components of the electric field $\vec{E}$ and the magnetic field $\vec{H}$, respectively. Each of the subscripts i,j denotes any of three Cartesian axes, and summation over repeated subscripts is understood. In the present paper these axes are taken to be the crystalline axes a,a',c of the tetragonal structure exhibited by $TbPO_4$ above its Néel temperature T_N. Use of the thermodynamic relations $\vec{P}=-\partial F/\partial\vec{E}$ and $\vec{M}=-\partial F/\partial\vec{H}$ in conjunction with Eq. (1) leads to

$$P_i=\alpha_{ij}H_j\ , \tag{2}$$

$$M_i=\alpha_{ji}E_j \tag{3}$$

for the components of the electric polarization $\vec{P}$ and the magnetization $\vec{M}$ which arise from linear ME effects. For later reference we further note that Eq. (1) yields

$$\alpha_{ij} = -\frac{\partial^2 F}{\partial E_i \partial H_j} \,. \tag{4}$$

and that thermodynamic as well as atomic theories of ME effects are reviewed elsewhere.[5]

To measure some of the components of $\overleftrightarrow{\alpha}$ we used high-aspect-ratio single crystals of $TbPO_4$ in the form of an elongated parallelepiped. In a typical crystal of this kind the long geometric axis is parallel to the crystallographic c axis, the short axes are parallel to the a and a' axes, and the a and a' faces (but not the c faces) are well formed. Unless stated to the contrary, the crystals were ME-annealed prior to all $\overleftrightarrow{\alpha}$ measurements in order to eliminate multiple antiferromagnetic domains and thus maximize the values of the components of $\overleftrightarrow{\alpha}$. The ME anneal consisted of cooling the crystals through T_N in the presence of an annealing electric field $\vec{E}_{an}$ and an annealing magnetic field $\vec{H}_{an}$. Both of these fields were applied parallel to the a axis because preliminary experiments led us to suspect that the magnetic symmetry of ME-annealed $TbPO_4$ is the same as that of ME-annealed $DyPO_4$ determined[6] earlier. E_{an} and H_{an} were turned off when the temperature T reached our lowest value (≈ 1.3 K) attained by pumping on liquid helium. Since the crystal thickness across the a faces (and also across the a' faces) is about 0.1 cm, we have $E_{an} \approx V_{an}/(300 \times 0.1)$ statvolts/cm, where V_{an} is the annealing voltage in volts.

To assess the effectiveness of the ME anneal, we observed, in an ME-annealed crystal, the magnetically induced ME effect described by Eq. (2). Specifically, we measured the static P_a induced by a static H_a. Using the static method described previously,[7,8] we determined P_a by measuring the static voltage V_a induced across the crystalline a faces. The experimental results presented in Figs. 1 and 2 show the values of P_a (in "arbitrary" units)

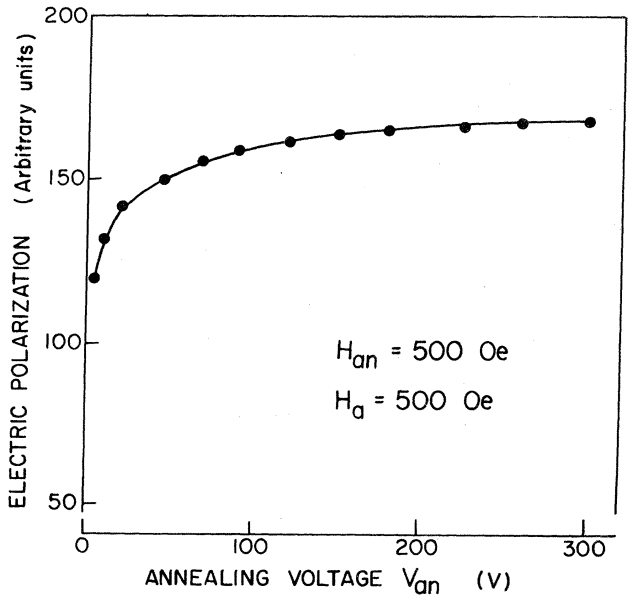

FIG. 1. Measured dependence of the electric polarization P_a, induced by a magnetic field $H_a = 500$ Oe, on the annealing voltage V_{an} for a fixed value $H_{an} = 500$ Oe of the annealing magnetic field.

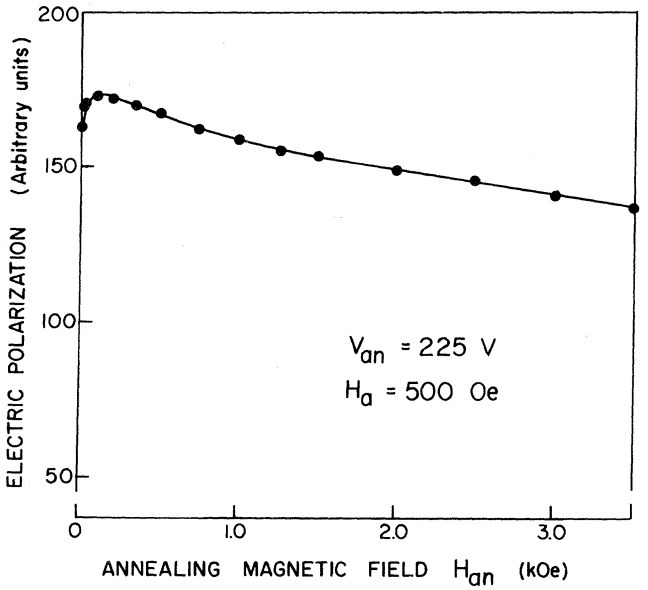

FIG. 2. Measured dependence of the electric polarization P_a, induced by a magnetic field $H_a = 500$ Oe, on the annealing magnetic field H_{an} for a fixed value $V_{an} = 225$V of the annealing voltage.

obtained by applying $H_a = 500$ Oe after repeated ME anneals. One arbitrary unit of P_a represents approximately 1 mV of V_a. In the data of Fig. 1, for each anneal, the value of H_{an} was fixed at 500 Oe, and V_{an} was fixed at a value in the range 0—300 V. In the data of Fig. 2 the value of V_{an} was kept constant at 225 V and H_{an} was fixed at a value in the range from 0 to about 3.5 kOe. Figure 1 shows that with increasing V_{an} the value of P_a increases monotonically and then approaches saturation. This behavior is similar to that found[9] in $DyPO_4$ and most probably indicates (since the ME anneal contributes an energy term proportional to $E_{an}H_{an}$) that the magnetic structure of the crystal approaches that of a single antiferromagnetic domain. With increasing H_{an}, on the other hand, P_a does not increase monotonically, but instead passes through a maximum, as shown in Fig. 2. A possible interpretation of this dependence is that the ionic magnetic moments of $TbPO_4$, unlike those of highly anisotropic (Ising-like) $DyPO_4$, are deflected by H_{an} toward the a axis even if the value of H_{an} is only a few kOe. On this basis it is understandable that the P_a values of $TbPO_4$ fail to reach saturation and ultimately decrease with increasing H_{an} even though the highest H_{an} values shown in Fig. 2 actually exceed those needed for achieving[9] saturation of P_a in $DyPO_4$.

We standardized the ME-annealing conditions to the values $V_{an} = 180$ V and $H_{an} = 500$ Oe which assure attainment, or near attainment, of the single-domain state without requiring that H_{an} be kept precisely at the value corresponding to the maximum of P_a. Using a crystal which had been subjected to this standard ME anneal we then measured, at $T = 1.94$ K, the dependence of the induced static P_a on the orientation of a static $\vec{H}$. The open and solid circles shown in Fig. 3 denote experimental data obtained by applying an $\vec{H}$ of magnitude 500 Oe at vari-

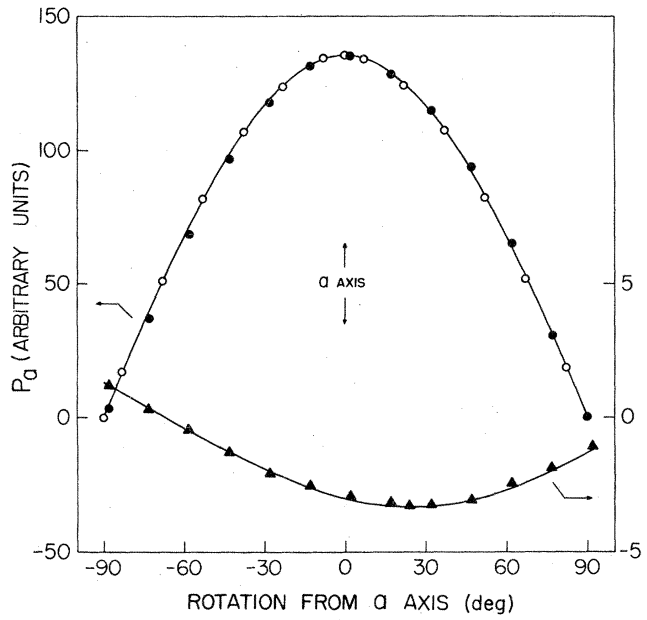

FIG. 3. Measured dependence of P_a in an ME-annealed crystal on the orientation of $\vec{H}$ in the a-a' plane (open circles) and in the a-c plane (solid circles). The triangles show an example of the measured dependence of P_a in a non-ME-annealed crystal on the orientation of $\vec{H}$ in either of these planes. The upper and lower curves are calculated as described in the text.

ous directions in the a-a' and a-c plane, respectively. The curve passing through these data is a normalized plot of the cosine of the angle between the a axis and the direction of $\vec{H}$. Because of the good agreement between the experimental points and this cosine curve, it is clear that in an ME-annealed crystal P_a depends solely on H_a. Stated equivalently, this means that $\alpha_{aa} \neq 0$ and $\alpha_{aa'} = \alpha_{ac} = 0$.

If the experiments discussed so far are repeated with the modification that E_{an} and H_{an} are applied along a' and the measurements are of $P_{a'}$ as a function of the orientation of $\vec{H}$, then the results are entirely analogous to those reported above. This was to be expected, of course, because the coolings involved in the ME anneals began at $T = 4.2$ K, i.e., at a temperature where $TbPO_4$ is known to be tetragonal so that a and a' are indistinguishable. From our measurements on elongated crystals we conclude, therefore, that in the a,a',c coordinate system $\overleftrightarrow{\alpha}$ is represented by the matrix

$$\underline{\alpha} = \begin{bmatrix} \alpha_{aa} & 0 & 0 \\ 0 & \alpha_{a'a'} & 0 \\ ? & ? & ? \end{bmatrix} . \tag{5}$$

We note that the $\underline{\alpha}$ of Eq. (5) refers to a crystal in which both E_{an} and H_{an} were applied along a or in which both E_{an} and H_{an} were applied along a'. The two above-mentioned ME-annealing experiments have verified the expected equality

$$|\alpha^a_{aa}| = |\alpha^{a'}_{a'a'}| , \tag{6}$$

where the superscript a denotes that E_{an} and H_{an} were both applied along a, and the superscript a' denotes that they were both applied along a'.

The result embodied in Eq. (5) is subject to the following limitations.

(i) The elements α_{ca}, $\alpha_{ca'}$, and α_{cc} of $\overleftrightarrow{\alpha}$ have not been measured because the elongated crystals are poorly formed, the c faces could not be ground, and hence P_c could not be determined.

(ii) The relative signs and magnitudes of α_{aa} and $\alpha_{a'a'}$ have not been ascertained because the quantities measured were only $|\alpha^a_{aa}|$ and $|\alpha^{a'}_{a'a'}|$. The two latter quantities resulted from different ME anneals and thus characterize different states of the crystal.

Both of these limitations were subsequently removed and thus a complete determination of $\overleftrightarrow{\alpha}$ was achieved, as described in Sec. III.

B. Symmetry of non-ME-annealed crystals

Before reporting on the magnitude and temperature dependence of α_{aa} in ME-annealed crystals, we briefly digress to consider the forms of $\overleftrightarrow{\alpha}$ in non-ME-annealed crystals. An example of our experimental data for such a crystal is the set of triangles shown in Fig. 3. The curve passing through the triangles is a normalized cosine curve whose phase was shifted with respect to that of the upper cosine curve in order to achieve agreement with experiment. In a non-ME-annealed crystal, therefore, P_a is induced not only by H_a but also by $H_{a'}$ or H_c, depending on whether the data denoted by triangles refer to a rotation of $\vec{H}$ in the a-a' plane or in the a-c plane. Thus the "a row" of $\overleftrightarrow{\alpha}$ in a non-ME-annealed crystal contains not only $\alpha_{aa} \neq 0$, but also $\alpha_{aa'} \neq 0$ and $\alpha_{ac} \neq 0$. We further note that upon successive coolings of a non-ME-annealed crystal through T_N, the dependence of P_a on the direction of $\vec{H}$ in the a-a' or a-c planes could always be described by a phase-shifted cosine curve. However, both the amplitude and phase of such a cosine curve had, in general, different values after each cooling.

Thus our ME experiments constitute a very simple method for demonstrating a fact which is known from neutron diffraction,[4] namely that the magnetic (and hence also the crystallographic) symmetry of non-ME-annealed $TbPO_4$ at temperatures below T_N is not tetragonal, but lower. Of particular interest is our result that the $\overleftrightarrow{\alpha}$ of ME-annealed crystals is reproducible from one cooling to the next, whereas the $\overleftrightarrow{\alpha}$ of non-ME-annealed crystals is not. This result suggests that the properties of ME-annealed crystals may be more fundamental than those of non-ME-annealed crystals.

C. Temperature dependence, magnitude, and atomic mechanism of α_{aa}

For the measurements of the T dependence of α_{aa} we replaced the above-mentioned static method by the previously described dynamic (1 kHz) methods[6] because the latter enabled us to determine this dependence more accurately even at temperatures where α_{aa} changes rapidly.

Although initially we had used the magnetically as well as the electrically induced ME effect, we confined the measurements to the electrically induced ME effect [Eq. (3)] after noticing that the coil producing the alternating magnetic field for the magnetically induced ME effect [Eq. (2)] generated enough heat to prevent the temperature from being controlled adequately. After turning off E_{an} and H_{an} at $T \approx 1.3$ K, we slowly increased the temperature by increasing the pressure of the helium vapor surrounding the $TbPO_4$ crystal.

The experimentally determined dependence of $|\alpha_{aa}|$ on T is shown in Fig. 4. In both parts of this figure the solid curve includes the temperature correction[10] arising from the height of the liquid-helium column, the so-called helium head correction, and the dashed curve represents the uncorrected experimental data temperatures (between 2.172 and 2.282 K) for which the helium head correction is non-negligible. As shown on the left-hand side of Fig. 4, the entire temperature range of the experiments is only about 1 K. Throughout this range the solid curve of $|\alpha_{aa}|$ is quite smooth and passes through a maximum before decreasing to zero near T_N. In contrast, the dashed curve of $|\alpha_{aa}|$ exhibits a discontinuity at T_λ (≈ 2.172 K), the λ point of helium, as shown most clearly on the right-hand side of Fig. 4 where the temperature scale is considerably expanded. Although the helium head correction may seem to be just an experimental detail, we mention it for two reasons. Firstly, it is a remarkable accident of nature that the T_N of $TbPO_4$ is exceedingly close to T_λ. Secondly, some of the early (non-ME) experiments on $TbPO_4$ resulted in values of T_N which differ by amounts exceeding the entire temperature range depicted on the right-hand side of Fig. 4.

By extrapolating, to $|\alpha_{aa}| = 0$, the linear portion of the solid $|\alpha_{aa}|$-vs-T curve in the vicinity of its turning point, we obtained

$$T_N = 2.276 \text{ K}, \tag{7}$$

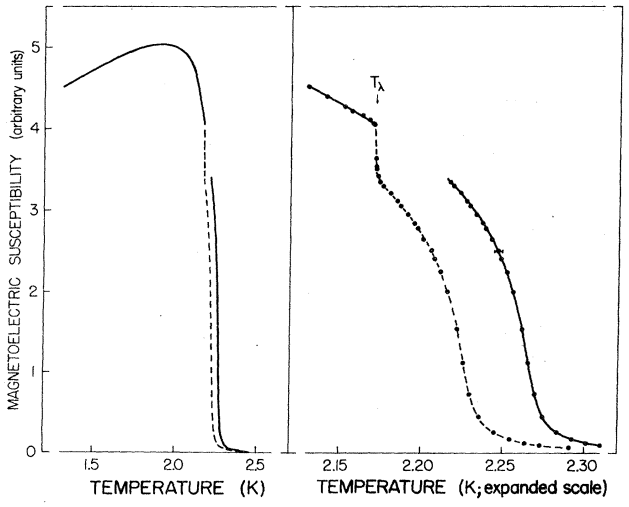

FIG. 4. Left-hand side: Measured temperature dependence of $|\alpha_{aa}|$. The helium head correction is included in the solid curve and omitted in the dashed curve. Right-hand side: Same as above but plotted on an expanded temperature scale.

which is in good agreement with the values $T_N = (2.29 \pm 0.1)$ and 2.28 K deduced, respectively, from subsequent magnetic and ME susceptibility measurements by England[2] and from recent neutron-diffraction experiments by Nägele *et al.*[4] It should also be mentioned that the possible uncertainties introduced by the helium head correction discouraged us from investigating critical phenomena by ME methods even though such an investigation[9] was successful in the case of $DyPO_4$.

Turning now to the magnitude of $|\alpha_{aa}|$, we found that its largest value is

$$|\alpha_{aa}|_{\max} = 1.1 \times 10^{-2}, \tag{8}$$

and it occurs at $T = (1.92 \pm 0.01)$ K. This value (which is dimensionless in the Gaussian units used) is considerably larger than any component of $\tilde{\alpha}$ reported for any material at any temperature. In particular, the $|\alpha_{aa}|_{\max}$ given by Eq. (8) exceeds, by an order of magnitude, the $|\alpha_{aa}|_{\max}$ of $DyPO_4$ which has the same (zircon) crystal structure as $TbPO_4$.

As stated in a review article,[11] but not published separately, the quantum-mechanical mechanism for α_{aa} proposed[12] in connection with $DyPO_4$ is also applicable to $TbPO_4$. This mechanism is described by a third-order perturbation energy which arises from the combined action of the odd part of the crystalline potential energy, the potential energy due to the applied electric field, and the Zeeman energy due to the applied magnetic field. In this perturbation the value of each of three important quantities (namely, the odd crystalline potential, the energy difference between the ground state and a state of opposite parity, and the energy difference between the ground state and the first excited state) is of the same order of magnitude in $TbPO_4$ as in $DyPO_4$. Our experimental result that $|\alpha_{aa}|$ in $TbPO_4$ is an order of magnitude larger than in $DyPO_4$ was explained[11] at least partially on the basis that the first excited state is the upper half of a Kramers doublet in $DyPO_4$ but not in $TbPO_4$. The underlying theoretical argument[11] is somewhat lengthy and we merely note that it does not involve the details of matrix elements but rests solely on the fact that the square of the time-reversal transformation is -1 for an odd number of electrons (as in Dy^{3+}), but is $+1$ for an even number of electrons (as in Tb^{3+}).

D. Switching, memory, and hysteresis

Figure 5 shows a recording of dynamically measured values of α_{aa} (in arbitrary units) as a function of a polarizing magnetic field H_c for a non-ME-annealed sample at $T = 1.94$ K. In discussing this figure we assume, without loss of generality, that the $TbPO_4$ crystal is in the state a and that is has just been exposed to a negative H_c. If we now apply a positive H_c, then α_{aa} follows the curve toward b where it decreases to zero if H_c is sufficiently large. Upon decreasing H_c to zero we find that α_{aa} changes its sign and follows the curve from b to c. Application of a negative H_c then causes α_{aa} to follow the solid curve cda. If, on the other hand, the original departure from the state a is initiated by negative values of H_c, then α_{aa} follows the dashed curve from a to d. Subsequent

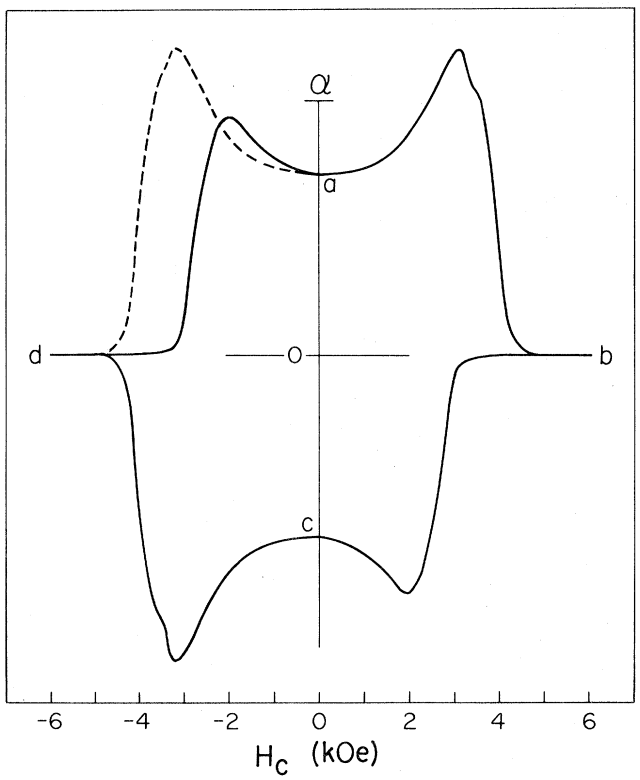

FIG. 5. Measured dependence of α_{aa} on a polarizing magnetic field H_c. The switching, memory, and hysteresis behavior shown here is described in the text.

reduction of the negative H_c to zero then reveals the presence of hysteresis by making α_{aa} follow the solid curve from d to a.

The switching and memory behavior described above is similar to that found[6] earlier in $DyPO_4$. There are, however, four differences between the switching and memory behavior of these two materials.

(1) In $TbPO_4$, unlike in $DyPO_4$, the top and bottom of the α_{aa}-vs-H_c plot are curved rather than flat, thus indicating the presence of nonlinear ME effects.

(2) The α_{aa} of $TbPO_4$, unlike that of $DyPO_4$, shows a switching and memory behavior accompanied by hysteresis effects.

(3) In $TbPO_4$, unlike in $DyPO_4$, we find that the behavior of α_{aa} is very similar (apart from small details) to that shown in Fig. 5 if the polarizing magnetic field is applied along the a or a' axis rather than along the c axis.

(4) The value of $|\alpha_{aa}|$ is zero polarizing field, i.e., at point a of Fig. 5, is an order of magnitude larger in switched $TbPO_4$ than in switched $DyPO_4$. Thus the $|\alpha_{aa}|$ of $TbPO_4$ exceeds that of $DyPO_4$ by about the same factor in the switched state as in the ME-annealed state.

III. MAGNETIC SYMMETRY

A. Crystal growth and sample preparation

Single crystals of $TbPO_4$ can be grown from fluxes of $Pb_2P_2O_7$ (Refs. 13 and 14) and PbO-PbF_2.[15] Both fluxes yield high-aspect-ratio crystals in the form of thin, elongated parallelepipeds with the c axis in the long direction and with well defined a and a' faces. Since this crystal morphology is unsuitable for attaching acceptable electrodes to c faces, it was necessary to synthesize crystals from which samples having adequate c faces could be prepared.

The $Pb_2P_2O_7$ flux was used to grow the crystals for the measurements described in Sec. II of this paper, and the PbO-PbF_2 flux was used to grow the crystals for those experiments of Sec. III in which we simultaneously determined the a row and the a' row of $\overleftrightarrow{\alpha}$ after a balanced ME anneal. The latter flux has the advantage of dissolving about 10 times as much rare-earth oxide as the former. In our original formulation of this flux, we used a $[PO_{2.5}]/[Pb^{2+}]$ ratio of unity, with a resultant excess of phosphate ion over that required to form the $TbPO_4$. We discovered, as Wanklyn[15] had previously, that a reduction in the amount of excess P_2O_5 favored the growth of crystals having aspect ratios close to unity. Accordingly, crystals used for those measurements of Sec. III of this paper which required adequate c faces (i.e., the determination of the c row of $\overleftrightarrow{\alpha}$) were grown from an equimolar PbO-PbF_2 flux with a $[Tb^{3+}]/[Pb^{2+}]$ ratio between 0.2 and 0.3 and a $[PO_{2.5}]/[Pb^{2+}]$ ratio between 0.89 and 0.97. Since there is some indication that Mo^{6+} may be incorporated into the lattice, Wanklyn's[15] procedure for substituting MoO_3 for some of the excess P_2O_5 was not used.

In preparing $TbPO_4$ crystals from $Pb_2P_2O_7$, we followed the procedure of Fiegelson.[13] In our procedure using the PbO-PbF_2 flux with reduced phosphate concentration, Tb_4O_7 was converted to $TbPO_4 \cdot H_2O$ by aqueous methods and dehydrated at elevated temperatures. The PbO, PbF_2, and $TbPO_4$ were premelted in Pt crucibles, excess P_2O_5 was then added, and the crucibles were then sealed in an inert atmosphere. (With the stoichiometric flux, Tb^{3+} was added either as Tb_4O_7 or as small crystals of $TbPO_4$ obtained from previous batches.) The oven temperature was held at 1260 °C, lowered to 1200 °C, then cooled slowly to 900 °C at 0.5 °C/h. This procedure yielded crystals which had not only adequate dimensions but had better mechanical and optical qualities than the crystals grown by our previous method.

A crystal sample having an aspect ratio of about unity is shown on the left-hand side of Fig. 6. Also shown are aluminum electrodes on the a and c faces and beveled edges which were ground on the sample to reduce the possibility of damage to the sample faces. On the right-hand side of Fig. 6 is shown similar information for a sample having a high aspect ratio. In this case, beveling of the edges was omitted because of the small size of the sample. During the ME measurements both types of samples were held within four rigid wire-electrode contacts retained with a Teflon ring. In ME-annealed samples we observed no effects which could be attributed to stress. In non-ME-annealed samples, of course, the possibility of stress effects cannot be excluded because the components of $\overleftrightarrow{\alpha}$ differed after each cooling, as mentioned in Sec. II B.

B. Balanced ME annealing and complete determination of $\overleftrightarrow{\alpha}$

By using in our static measurements of the magnetically induced ME effect the type of sample depicted on the

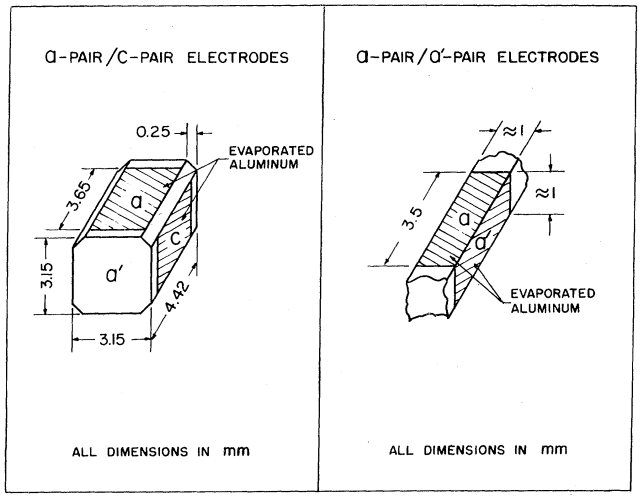

FIG. 6. Shape and dimensions of crystal samples having a low (left-hand side) and high (right-hand side) aspect ratio.

right-hand side of Fig. 6, i.e., a sample equipped with both an a pair and an a' pair of electrodes, we were able to measure the a row and a' row of $\vec{\vec{\alpha}}$ simultaneously. In particular, we determined simultaneously the α_{aa} and $\alpha_{a'a'}$ resulting from a given ME anneal. We observed that the sign of $\alpha_{a'a'}$ is the opposite of that of α_{aa}, and thus we removed part of the limitation (ii) contained in Sec. II A. However, we found that $|\alpha_{aa}|$ and $|\alpha_{a'a'}|$ are unequal, and that $|\alpha_{aa}|$ is larger or smaller than $|\alpha_{a'a'}|$ depending on whether or not the E_{an} and H_{an} of the ME anneal preceding the measurement had been applied along the a or a' axis.

To overcome limitation (ii) we introduced the "balanced" ME-annealing method characterized by the configuration of electrodes and annealing fields shown in Fig. 7. It is seen that we applied $\vec{E}_{an}$ (using $V_{an}=225$ V) at $+45°$ and $\vec{H}_{an}$ (using $H_a=707$ Oe) at $-45°$ with respect to the a axis of a crystal of square cross section. Before explaining the advantages of this arrangement we note that in the a,a',c coordinate system Eq. (1) has the form

$$F=-\alpha(E_aH_a-E_{a'}H_{a'}) \tag{9}$$

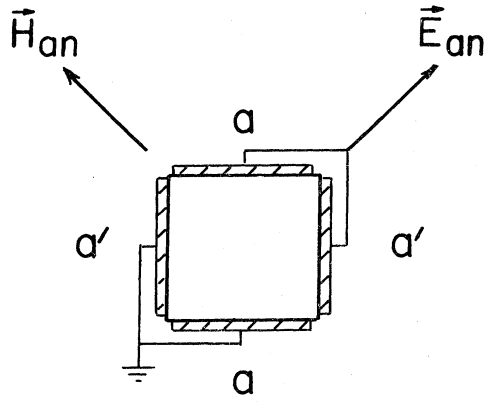

FIG. 7. Configuration of electrodes and annealing fields used in the balanced ME anneal.

for crystals whose magnetic symmetry group is $4'/m'mm'$. This symmetry is known[6] to apply to $DyPO_4$, and, as shown below, is now found to apply to $TbPO_4$ as well. The ME susceptibility α appearing in Eq. (9) is free of subscripts because it is the single independent component of the $\vec{\vec{\alpha}}$ allowed by the symmetry $4'/m'mm'$. For our discussion of ME annealing we now add the subscript "an" to all quantities (except α) appearing in Eq. (9) to obtain

$$F_{an}=-\alpha(E_{an,a}H_{an,a}-E_{an,a'}H_{an,a'}) . \tag{10}$$

This equation clearly shows that with the configuration of $\vec{E}_{an}$ and $\vec{H}_{an}$ used in the balanced ME anneal, the a and a' directions are treated equivalently, whereas in the "ordinary" ME anneal described in Sec. II A, the a direction (or the a' direction) is treated preferentially.

Figure 8 shows the experimental results obtained at $T=1.94$ K on the type of sample shown on the right-hand side of Fig. 6 after subjecting it to a balanced ME anneal. The measured values of P_a plotted on the left-hand side of Fig. 8 were induced by applying $\vec{H}$ successively in the a-c plane (top), the a'-c plane (center), and the a-a' plane (bottom). Corresponding values of $P_{a'}$ were

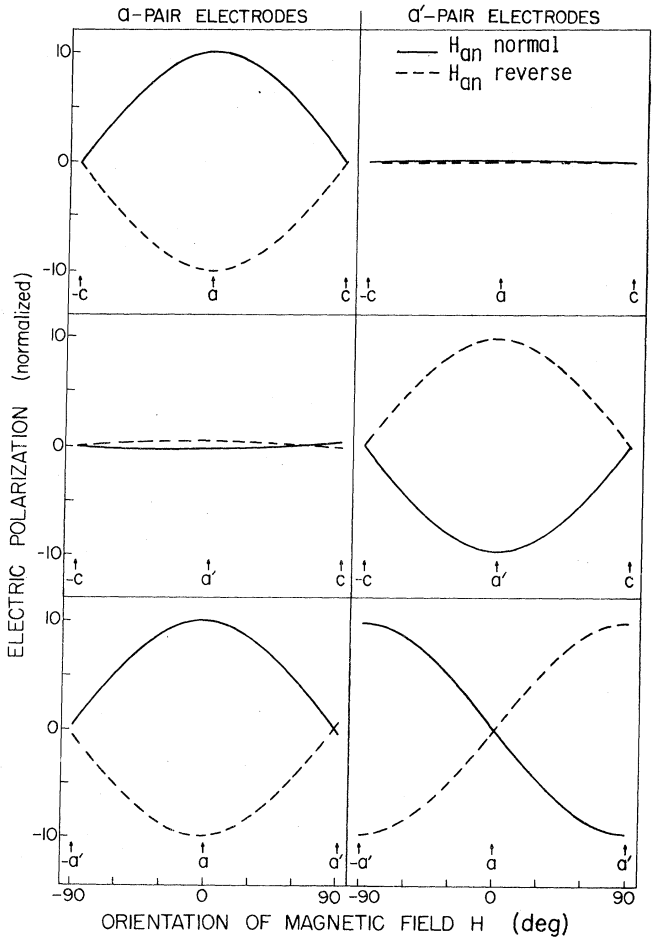

FIG. 8. Dependence of P_a (left-hand side) and $P_{a'}$ (right-hand side), measured simultaneously after a balanced ME anneal on the orientation of $\vec{H}$ in the a-c plane (top), a'-c plane (center), and a-a' plane (bottom).

measured simultaneously with P_a and are plotted on the right-hand side of the figure. Each of the six parts of Fig. 8 contains two graphs, one corresponding to $\vec{H}_{an}$ in the "normal" direction (solid line) and one corresponding to $\vec{H}_{an}$ in the "reverse" direction (dashed lines). The polarization values represented by these two graphs differ only in sign, as expected from Eq. (10).

Next we interpret Fig. 8 in a manner analogous to that used in connection with the open and solid circles of Fig. 3. In this way we obtain the results

$$\alpha_{aa} \neq 0 , \tag{11}$$

$$\alpha_{aa'} = \alpha_{ac} = \alpha_{a'a} = \alpha_{a'c} = 0 , \tag{12}$$

$$\alpha_{a'a'} = -\alpha_{aa} . \tag{13}$$

Apart from experimental errors arising from imperfect sample alignment, Eqs. (11) and (12) merely confirm the results contained in Eq. (5). In contrast, Eq. (13) is new and expresses the desired removal of limitation (ii) contained in Sec. II A.

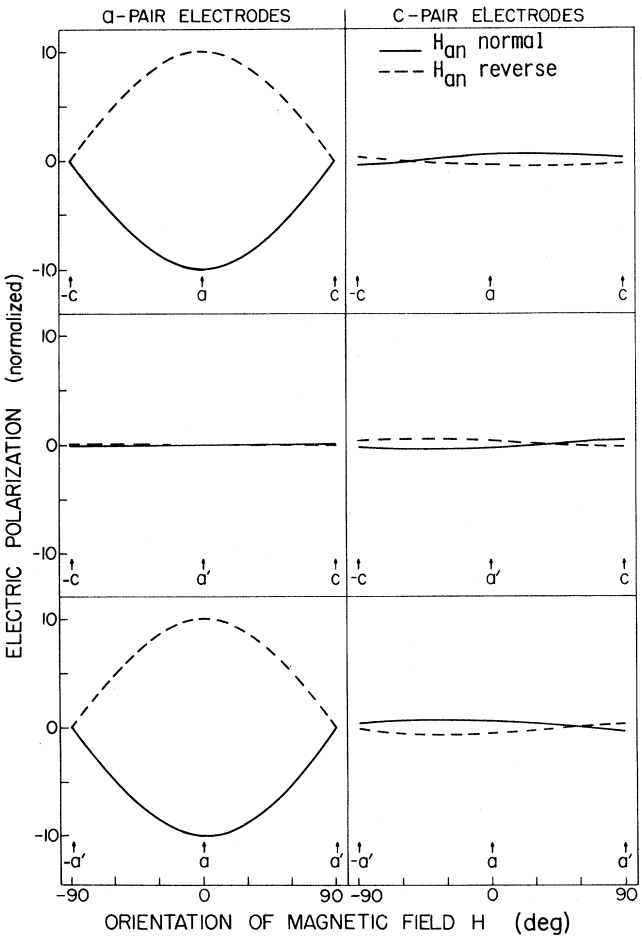

FIG. 9. Dependence of P_a (left-hand side) and P_c (right-hand side), measured simultaneously after an ordinary ME anneal, on the orientation of $\vec{H}$ in the a-c plane (top), a'-c plane (center), and a-a' plane (bottom).

The experimental results shown in Fig. 9 were obtained at $T = 1.94$ K on the type of sample shown on the left-hand side of Fig. 6 after subjecting it to an ordinary ME anneal. Since the use of a balanced ME anneal would have introduced various experimental complications, it is fortunate that apart from experimental errors the measured values of P_c, shown on the right-hand side of Fig. 9, are found to be zero for all orientations of $\vec{H}$. Thus we removed limitation (i) contained in Sec. II A and obtained

$$\alpha_{ca} = \alpha_{ca'} = \alpha_{cc} = 0 , \tag{14}$$

as anticipated by our assumption that the magnetic point group of ME-annealed $TbPO_4$ is $4'/m'mm'$. The left-hand side of Fig. 9 contains the results of a "control" experiment in which P_a was measured simultaneously with P_c. It is seen that these P_a values agree, except for a change in sign, with those shown on the left-hand side of Fig. 8, even though the measurements of the former P_a values were preceded by an ordinary ME anneal and those of the latter were preceded by a balanced ME anneal. Such a change in sign is quite possible because the absolute sign of a component of $\vec{\alpha}$ cannot be determined by ME measurements, and also because the $+a$ and $-a$ directions cannot be distinguished in either sample. It should also be noted that the principal errors in the data of Fig. 9 arise not only from imperfect sample orientation, as in Fig. 8, but also from the fact that the beveled portions of the sample used for Fig. 9 cause the effectiveness of the ME anneal to diminish.

By combining Eqs. (11)–(15), our final result for the form of $\vec{\alpha}$ can be expressed by the matrix

$$\underline{\alpha} = \begin{bmatrix} \alpha & 0 & 0 \\ 0 & -\alpha & 0 \\ 0 & 0 & 0 \end{bmatrix} , \tag{15}$$

where the symbol α appearing in the diagonal is simply an abbreviation for α_{aa}. This form is just what one obtains by using Eq. (4) in conjunction with Eq. (9), an equation based on the symmetry $4'/m'mm'$. More generally, the form of $\vec{\alpha}$ given by Eq. (15) corresponds not only to the symmetry $4'/m'mm'$ but also to four additional tetragonal symmetries listed on p. 138 of Birss.[15] The crystallographic point groups associated with these four tetragonal symmetries lack the inversion operation, and hence they describe a *crystal* structure which is distorted compared to the $4/mmm$ symmetry exhibited by $TbPO_4$ for $T > T_N$. Since we observed no experimental indication of a distortion for $T < T_N$, we disregard the four above-mentioned tetragonal symmetries and adopt $4'/m'mm'$ as the magnetic symmetry of ME-annealed $TbPO_4$ for $T < T_N$. This is supported by the results of neutron-diffraction experiments[4] which show that, even in non-ME-annealed $TbPO_4$, the transition at $T = T_N$ is purely magnetic, and that for $2.15 < T < 2.28$ K the ionic magnetic moments are along the c axis.

We conclude from Sec. III that with the use of a bal-

anced ME anneal, the magnetic symmetry of ME-annealed $TbPO_4$ was determined to be $4'/m'mm'$ within experimental error. A given ordinary ME anneal, on the other hand, led to $\alpha_{aa} \neq \alpha_{a'a'}$, as stated near the beginning of Sec. III B, and thus to orthorhombic symmetry. It is clear, therefore, that the balanced ME anneal suppresses the low-symmetry lattice distortions reported[4] to exist in non-ME-annealed $TbPO_4$ at 2.15 K. In other words, the balanced ME anneal imposes a tetragonal symmetry and "freezes" it below the Néel temperature.

---

*Present address: Department of Physics, The Johns Hopkins University, Baltimore, MD 21218.

[1]G. T. Rado and J. M. Ferrari, in *Magnetism and Magnetic Materials—1972 (Denver),* Proceedings of the 18th Annual Conference on Magnetism and Magnetic Materials, edited by C. D. Graham and J. J. Rhyne (AIP, New York, 1973), p. 1417.

[2]N. England, Ph.D. thesis, University of Oxford, 1978.

[3]G. T. Rado, J. M. Ferrari, and W. G. Maisch, J. Appl. Phys. 53, 8151 (1982).

[4]W. Nägele, D. Hohlwein, and G. Domann, Z. Phys. B 39, 305 (1980) and references quoted therein to the older $TbPO_4$ literature.

[5]G. T. Rado, Int. J. Magn. 6, 121 (1974).

[6]G. T. Rado, Phys. Rev. Lett. 23, 644 (1969); 23, 946(E) (1969).

[7]G. T. Rado, in *Proceedings of the International Conference on Magnetism, Nottingham, 1964* (IOP, London, 1965), p. 361.

[8]G. T. Rado and J. M. Ferrari, Phys. Rev. B 12, 5166 (1975); 14, 4239(E) (1976).

[9]G. T. Rado, Solid State Commun. 8, 1349 (1970); 9, vii(E) (1971). This reference contains mostly ME studies of critical behavior in $DyPO_4$ but briefly mentions the results of ME annealing experiments. Additional ME annealing experiments performed by G. T. Rado and J. M. Ferrari (unpublished).

[10]See, for example, F. G. Brickwedde, H. van Dijk, M. Durieux, J. R. Clement, J. K. Logan, *The 1958 He^4 Scale of Temperatures,* National Bureau of Standards Monograph No. 10 (U.S. GPO, Washington, D.C., 1960), Table V.

[11]See Ref. 5, pp. 127—129 and appendix therein.

[12]See Ref. 6 and the improved numerical estimate given in Ref. 5.

[13]R. S. Feigelson, J. Am. Ceram. Soc. 47, 257 (1964).

[14]S. H. Smith and B. M. Wanklyn, J. Cryst. Growth 21, 23 (1974).

[15]R. R. Birss, *Symmetry and Magnetism* (North-Holland, Amsterdam, 1964), p. 138.